# Biaxial mechanical behavior of excised porcine mitral valve leaflets

KAREN MAY-NEWMAN AND FRANK C. P. YIN
*Division of Cardiology, Department of Medicine and Department of Biomedical Engineering, Johns Hopkins School of Medicine, Baltimore, Maryland 21205*

**May-Newman, Karen, and Frank C. P. Yin.** Biaxial mechanical behavior of excised porcine mitral valve leaflets. *Am. J. Physiol.* 269 (*Heart Circ. Physiol.* 38): H1319–H1327, 1995.—Anterior and posterior leaflets from excised porcine mitral valves were mechanically tested under cyclic equibiaxial and strip biaxial stretch protocols at a strain rate of 4–12%/s after preconditioning. Cauchy stress and Lagrangian strain were calculated for both membrane and three-dimensional cases. The leaflets exhibited nonlinearly elastic, anisotropic behavior. Both anterior and posterior leaflets were less extensible in the circumferential than in the radial direction under equibiaxial stretch, with stress ratios of 5.7 and 4.3, respectively. The posterior leaflets exhibited greater extensibility in both directions and lower circumferential posttransitional moduli (ranges 690–820 vs. 2,500–3,200 N/m for anterior). This larger posterior extensibility may be due to the greater number of chordal attachments, which provide additional mechanical stability to this structure. Coupling of radial and circumferential mechanical behavior was evidenced by the response to different stretch protocols, indicating a complex microstructural coupling between individual collagen fibers or bundles. These are the first biaxial data for mitral valves and are a foundation for the development of a more detailed quantitative material description.

stress; strain; anisotropy; material properties

THE MITRAL VALVE APPARATUS prevents backflow of blood from the left ventricular chamber as the heart contracts. It consists of the mitral annulus, from which arise two membranous leaflets connected to papillary muscles by a series of chordae tendineae. The entire apparatus must resist high physiological pressures of 100–200 mmHg for several billion cycles during a normal lifetime, thus requiring high mechanical durability (22). An understanding of local stresses in the normal valve leaflets may provide insight into mechanisms for pathological structural remodeling such as fibrosis, myxomatous change and calcification. Because stress cannot be measured directly in a reliable manner in the valve, procedures such as the finite element method will be required to accurately estimate the stress distribution. This requires quantitative information on tissue microstructure, material behavior, loading conditions, and in vivo deformation.

Critical to the above is an accurate description of material behavior. Experimental testing is necessary to provide data for the formulation of a constitutive relation, a quantitative description of the dependence of tissue stress on strain or deformation. Previous uniaxial studies have provided some information on the behavior of mitral valve tissue (4, 11, 16) but not sufficient data to describe in detail its properties under multiaxial loading. Data from multiaxial tests are thus required.

Valve leaflets are thin and nearly incompressible; therefore biaxial data are useful for studying their biomechanical behavior. In this study, the biaxial testing of individual porcine mitral valve leaflets was performed under a variety of loading protocols. The general mechanical behavior is identified and comparisons made between biaxial and uniaxial loading responses. These data are the foundation for an accurate, quantitative description of mitral tissue behavior.

## METHODS

*Specimen preparation.* Previous studies have demonstrated that both size (15) and microstructural composition (6) are similar for both human and porcine mitral valves. Therefore, due to the limited availability of human tissue, porcine valves were used. Mitral valves were obtained from the hearts of 29 large (25–45 kg) adult pigs. The individual leaflets were separated and trimmed to approximate a rectangular shape, leaving the chordae tendineae and a small portion of the annulus intact (see Fig. 1). Leaflets $< 1$ cm$^2$ were discarded. Four small markers (150–200 μm) demarcating a small quadrilateral in the central region were glued to the leaflet surface with a small drop of cyanoacrylate adhesive (Krazy-glue, Borden). The specimen was mounted in trampoline fashion on a biaxial testing device so that the circumferential and radial directions were aligned with the $x$ and $y$ axes of mechanical testing, respectively. Four to six continuous stitches with 5–0 silk suture were placed on each of three sides of the leaflet specimen. For the anterior leaflets, the free edge was tethered by tying loops to four to five individual chordae when their geometry was suitable and suturing the loops to the biaxial apparatus to simulate the in vivo attachments. This arrangement was true for the majority of the anterior mitral leaflets, which displayed several prominent (0.5-mm wide) chordae oriented perpendicular to the free, or coapting, edge of the leaflet. If the arrangement of chordae was not suitable, this edge of the tissue was attached like the other sides. Identical protocols in three anterior leaflets under both conditions were performed to examine whether the chordae or the suture-tethering scheme influenced the measured results. In the posterior leaflets the free edge was sutured similarly to the other three sides.

The valve was superfused during testing with an isotonic saline solution (0.9%) at room temperature (25–28°C). Because of the length of time required for testing each leaflet, it was sometimes necessary to store the leaflet for 1–3 days in cold (4°C) penicillin-doped (1 ml/75 ml) normal saline before testing, which usually occurred within 24 h. The effect of saline storage on mechanical properties was examined in two anterior and two posterior leaflets. Leaflets were tested fresh, at 1 day, and at two other times up to 8 days. The sutures and markers were kept intact to facilitate specimen mounting and repeated testing.

*Experimental protocol.* The biaxial testing device for large specimens described previously (3) was adapted to test the small (1–4 cm$^2$) specimens by using small markers (150–200 μm), setting the camera magnification so that resolution was

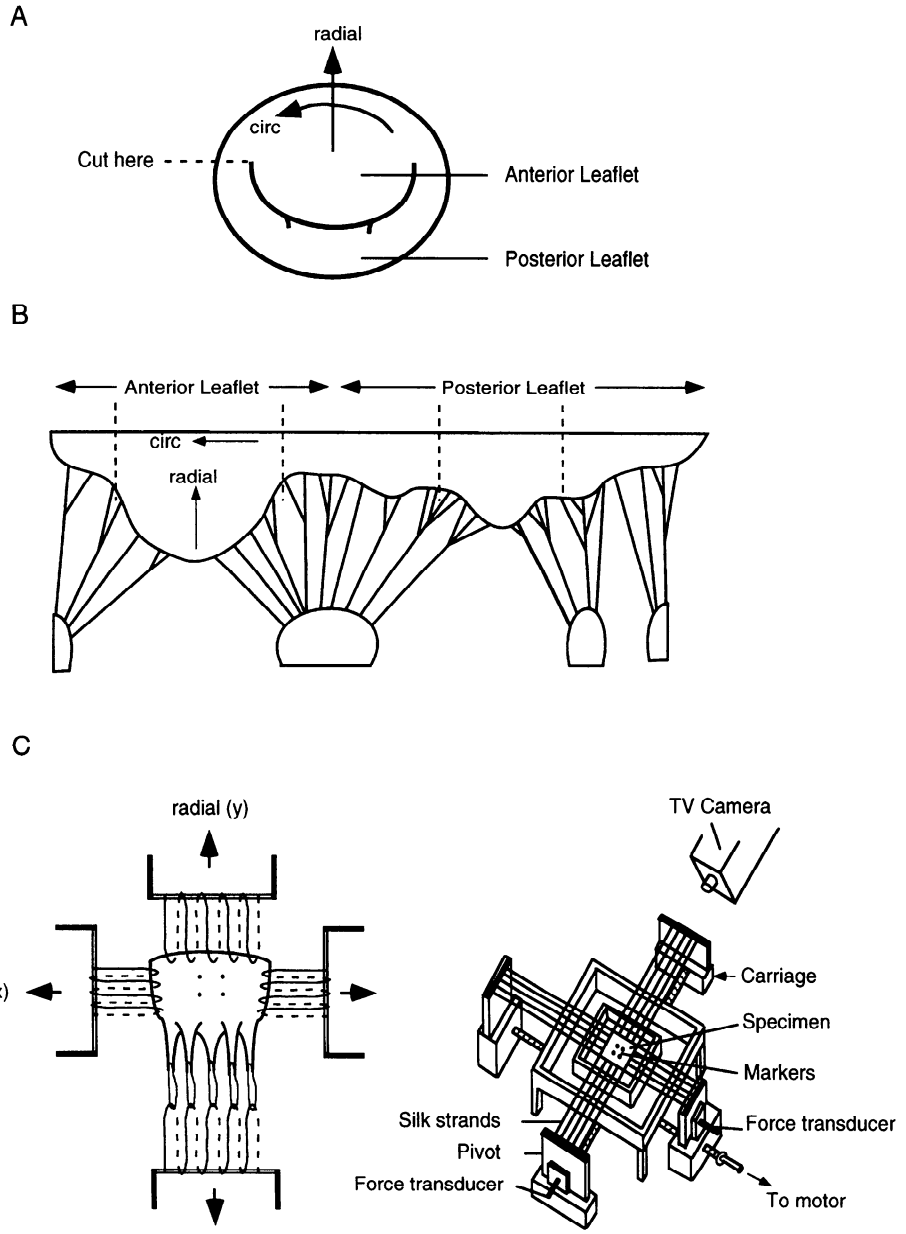


Fig. 1. Mitral leaflet specimen preparation. *A*: intact mitral annulus is trimmed 2–3 mm outside muscle-leaflet interface. Original polar coordinate system with circumferential (circ) and radial axes is shown. A single cut (dotted line) is made at one commissure, and chordae and papillary muscles are isolated from left ventricular wall. *B*: schematic of excised valve, indicating coordinate axes and approximate location of cuts for isolation of individual leaflet specimens. Chordae tendineae are cut near papillary muscle insertion sites. *C*: isolated leaflet specimen is oriented such that circumferential and radial directions correspond to axes of mechanical testing. Each carriage of the biaxial apparatus was tethered with one continuous suture.

68 pixels/mm, and increasing the force resolution to 3 analog-to-digital units/g. These modifications produced a central measurement area of 5–15% of the total, providing acceptable freedom from edge and/or tethering effects (29). The loading mechanism stretched the tissue in two orthogonal directions and was controlled according to a prescribed waveform using dimensions obtained from a video system that continuously tracked the $x$ and $y$ coordinates of the four markers (8). The tissue was stretched until it exhibited rapid stiffening in both directions. The specimens were not stretched beyond this point to minimize irreversible tissue damage, which was suspected if the mechanical responses were not repeatable. Cyclic stretching was applied as displacement ramps with a period of 10 s, corresponding to a strain rate of 4–12%/s or 3–10 mm/min.

The leaflet specimen was preconditioned for 8–10 cycles to establish a repeatable force-extension curve for each protocol. The stress-free reference dimensions, $D_x$ and $D_y$, of the central marker region were obtained by removing all external loads and allowing the tissue specimen to float on the surface of the saline bath. An equibiaxial stretch protocol was applied first, followed by a strip biaxial test in each of the circumferential and radial directions, respectively. A strip biaxial test is essentially a uniaxial test and consists of holding one direction at its unloaded dimension while stretching the specimen in the other direction. The prescribed stretch values were determined and controlled based on the average distance between the two pairs of markers in each direction. The $x$ and $y$ coordinates of the four marker centroids together with the corresponding force measurements were digitized at 30 Hz and stored on a 386PC. The unloaded dimension was monitored throughout the experiment to determine if any viscoelastic or irreversible changes had occurred. At the conclusion of the experiment, the specimen was unloaded, and the length along each side over which the force was applied, $L_x$ and $L_y$, was measured as the distance between the two outermost sutures. Thickness, $t$, was measured in the central region with dial calipers (Manostat) three times and averaged for each specimen.

*Stress and strain calculations.* Strain in the central region was calculated from the $x$ and $y$ coordinates of the four markers in the unloaded reference state and subsequent

loading states using the method described by Humphrey, et al. (13). Circumferential and radial stretch ratios are the normal components of the deformation gradient tensor **F**, which includes shearing; however, the shear terms were found to be negligible. Green's strain, **E**, is computed from **F** as

$$\mathbf{E} = \frac{1}{2}(\mathbf{F}^{\mathrm{T}}\mathbf{F} - \mathbf{I}) \quad (1)$$

where **I** is the identity tensor. Cauchy stress **T** is calculated from the first Piola-Kirchoff stress **P**, the applied force acting on the undeformed area as

$$\mathbf{T} = \frac{1}{J}(\mathbf{F}\cdot\mathbf{P}) \quad (2)$$

where $J$ is the Jacobian, or determinant of **F** ($det\mathbf{F}$). Both membrane (two-dimensional) and three-dimensional (utilizing thickness and invoking incompressibility) approaches were employed to analyze and compare the data. Cauchy stress (three-dimensional) for the plane stress situation is equivalent to the membrane stress (two-dimensional) normalized by the deformed leaflet thickness. Data were filtered numerically, using a running median of span 15 and the number of data points reduced to 50 points/curve. For each valve leaflet, a membrane and three-dimensional stress-strain plot was made for each direction.

Despite the care taken to accurately measure the unloaded reference state and to control deformation to produce an equibiaxial mechanical test, small errors in the identification of the marker position (0.05 mm) translated to slight errors in the applied stretch protocol (5%). Consequently, tests were excluded if the equibiaxial stretch ratios varied by more than 10% from each other.

*Material indexes.* Because all the stress-strain relations consisted of a large strain range of high extensibility followed by a transition with rapid stiffening, we chose simple indexes to describe the data, approximating the nonlinear response with a bilinear relation. For comparisons with previous reports we chose an index of leaflet extensibility in the region following the transition point to be $\lambda^*$, the stretch at a common stress value of 20 N/m $T^*$ (see DISCUSSION for the rationale for this choice), for all leaflet specimens. Elastic moduli for the pre- and posttransitional regions of the nonlinear stress-strain curve were defined as the tangent stiffness at $0.5\lambda^*$ and $\lambda^*$, respectively. Curve fits to at least 50 points of data using both exponential and fourth-order polynomial functions were performed following previous methods (16, 25). The best fit was then differentiated, and the function was evaluated at $\lambda^*$ and $0.5\lambda^*$. For the membrane analysis, these moduli were denoted as $M_{pre}$ and $M_{post}$, and for the three-dimensional analysis they were denoted as $E_{pre}$ and $E_{post}$.

An index of material anisotropy, $R$, was defined as the ratio of circumferential to radial stress during equibiaxial loading using a linear regression to the data (32). A value of unity indicates isotropic behavior.

*Statistical analysis.* Statistical comparison of the various indexes was performed using paired $t$-tests between circumferential and radial properties in the anterior and posterior groups separately. Unpaired $t$-tests were used to compare anterior and posterior leaflets. Significance was accepted at $P \leq 0.05$. Comparisons with $P < 0.001$ were considered highly significant.

*Tethering effects.* The influence of the tethering method on the stress-strain relationship is shown for a representative specimen in Fig. 2. Qualitatively, the figure shows that these relationships are similar for the protocol performed with leaflet tethered by the chordae vs. directly sutured to the tissue. $\lambda^*$ for the three specimens demonstrated a 0.2% difference in the circumferential direction and a 5% difference in the radial direction. Pre- and posttransitional elastic moduli differed by $<10\%$, indicating no appreciable difference between these two tethering methods.

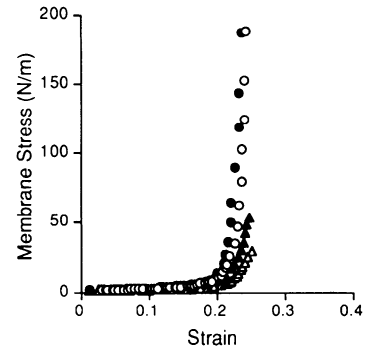


Fig. 2. Comparison of tethering methods in one anterior leaflet. An equibiaxial stretch protocol was repeated for tethering of biaxial specimen to apparatus by individual chordae (open symbols) and direct suturing (filled symbols). Circles, circumferential direction; triangles, radial direction.

*Saline storage effects.* Results demonstrating the effect of saline storage are shown in Fig. 3. Four leaflets were tested and extensibility indexes pooled for different time points, although all leaflets were not tested at each time point. Small and inconsistent changes were observed over time. After one

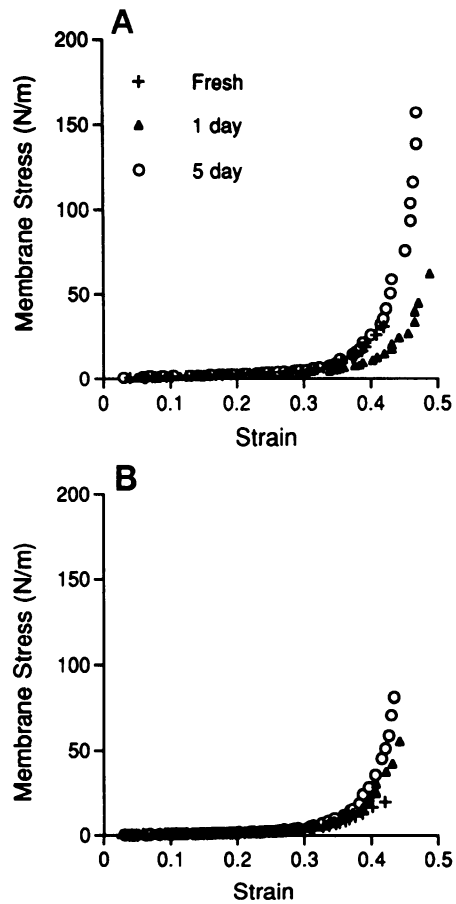


Fig. 3. Effect of saline storage on stress-strain response in circumferential ($A$) and radial directions ($B$) in a posterior leaflet specimen. Changes were small and inconsistent, indicating no significant alteration in mechanical properties up to 5 days after excision.

Table 1. *Leaflet specimen characteristics*

| Leaflet | $n$ | $t$, mm | $L_x$, mm | $L_y$, mm | $D_x$, mm | $D_y$, mm | $f_a$, % |
|---|---|---|---|---|---|---|---|
| Anterior | 19 | 0.69 ± 0.26 | 12.52 ± 3.72 | 7.72 ± 2.05 | 2.80 ± 0.95 | 2.03 ± 0.49 | 6.68 ± 3.58 |
| Posterior | 13 | 0.51 ± 0.14 | 10.21 ± 3.31 | 7.69 ± 1.77 | 2.49 ± 0.84 | 1.79 ± 0.45 | 5.83 ± 1.79 |

Values are means ± SD. $n$, No. of specimens; $t$, thickness; $L_x$ and $L_y$, length along each side over which force was applied in $x$ and $y$ directions, respectively; $D_x$ and $D_y$, stress-free reference dimensions in $x$ and $y$ directions, respectively; $f_a$, area demarcated by the four markers, as a percentage of total area of specimen.

day of saline storage, $\lambda^*$ in the circumferential and radial directions increased by 5.9% and 5.1% compared with freshly excised tissue, respectively. A further increase of 8.5% (circumferential) and 0.3% (radial) was noted after 3 days, a 10–11% decrease (both directions) was observed after 5 days, and slight increase (4–5%) was noted by 8 days. There was no consistent trend to suggest a progressive structural degradation; instead the variations most likely reflect variability in our ability to measure the unloaded reference state.

## RESULTS

Twenty-eight anterior and fifteen posterior leaflets were tested by the above protocol. Ten leaflets were excluded from data analysis: seven (5 anterior and 2 posterior) did not meet the equibiaxial test criteria, one ripped during testing, and two did not have sufficient data for analysis (i.e., $T_{max} << T^*$, where $T_{max}$ is the maximum value of **T** for a particular protocol). The dimensions of the leaflet specimens and central test regions are summarized in Table 1 for 19 anterior and 13 posterior leaflets, respectively. On average, anterior leaflets were larger than posterior leaflets. The central region of all specimens demarcated by the four markers occupied 2–15% of the total area ($f_a$, Table 1). Previous finite-element studies by Nielson (29) suggest that this area fraction of a biaxially loaded tissue specimen is small enough to be essentially free from edge effects due to specimen tethering. In eight specimens, unloaded dimensions were recorded before and after the study. Referring strains to the initial unloaded dimensions, we found the reference state to be repeatable within 2%.

*Equibiaxial tests.* Both anterior and posterior leaflets behaved anisotropically, as shown in Fig. 4, which depicts the loading portion of the circumferential and radial membrane stress-strain relationships of a typical valve under equibiaxial stretching. The stress-strain relations are highly nonlinear, as is characteristic of most soft biological tissues. All tissues demonstrated essentially full elastic recovery at the strain rate tested following preconditioning and exhibited some hysteresis (Fig. 5). In general, the circumferential and radial curves initially followed the same relation, whereas the transition to the steeper linear stress-strain region occurred at lower strains in the circumferential direction. Conversely, the observed transition occurred more gradually and at higher strains in the radial direction.

Equibiaxial test results for all leaflets are summarized in Table 2. In the anterior leaflets, $\lambda^*$ is significantly smaller in the circumferential (1.174) compared with the radial direction (1.202), demonstrating greater extensibility in the radial direction ($P < .0001$). Correspondingly, both $M_{pre}$ and $M_{post}$ were larger in the circumferential (51.1 and 2,558 N/m) than radial directions (27.4 and 801 N/m), indicating anisotropy, with the differences more pronounced in the posttransitional region. The value of $R$ was 5.71 for the anterior leaflets, indicating that stress along the circumferential axis was five to six times greater than the corresponding radial stress at the same strain. Although 13 of the leaflets exhibited a slight concavity towards the circumferential stress axis, a constant ratio was a reasonable approximation for the relationship. The regression correlation coefficients for all leaflet specimens were $> 0.95$.

The posterior leaflet exhibited more isotropic material behavior, with $\lambda^*$ nearly equal in the circumferential and radial directions (1.234 and 1.242, respectively). The value of $R$ was 4.27, slightly, but not significantly, lower than the anterior leaflets. Otherwise the circumferential-radial differences of the posterior leaflets were similar to those of the anterior leaflets.

The anterior leaflets were significantly less extensible along the circumferential direction than the posterior leaflets, as demonstrated by $\lambda^*$ values of 1.174 vs. 1.234,

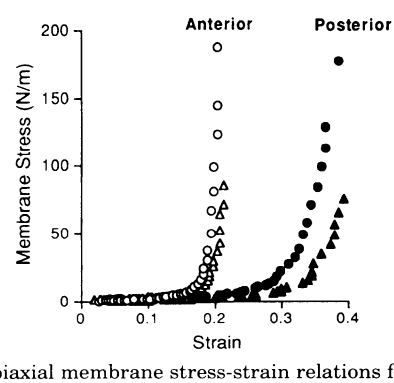


Fig. 4. Equibiaxial membrane stress-strain relations from both anterior (open symbols) and posterior (filled symbols) leaflets. Circles, circumferential direction; triangles, radial direction.

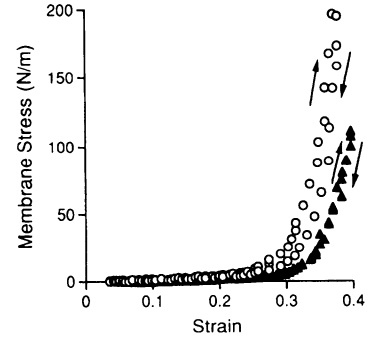


Fig. 5. One cycle of equibiaxial loading in a posterior leaflet. Direction of arrows indicates loading (*up*) and unloading (*down*) portions. Valve leaflets exhibit slight hysteresis under cyclic loading. Circles, circumferential direction; triangles, radial direction.

Table 2. *Summary of material indexes*

| Leaflet | Protocol | Direction | $\lambda^*$ | $M_{pre}$, N/m | $M_{post}$, N/m | $E_{pre}$, kPa | $E_{post}$, kPa | $R$ |
|---|---|---|---|---|---|---|---|---|
| Anterior | Equi | Circ | $1.174 \pm .044^{b,c,e}$ | $51.1 \pm 38.3^{a}$ | $2,558 \pm 1,582^{b,d}$ | $89.3 \pm 91.7$ | $8,960 \pm 8,830^{a,c}$ | $5.71 \pm 4.38$ |
| | | Rad | $1.202 \pm .049^{e}$ | $27.4 \pm 11.2^{c,f}$ | $801 \pm 369^{e}$ | $60.5 \pm 43.8$ | $2,400 \pm 1,480$ | |
| | Strip | Circ | $1.183 \pm .046^{a,d}$ | $50.9 \pm 40.8^{a}$ | $3,156 \pm 3,397^{a,c}$ | | | |
| | | Rad | $1.340 \pm .153^{c}$ | $18.8 \pm 7.3^{c}$ | $360 \pm 325$ | | | |
| Posterior | Equi | Circ | $1.234 \pm .062^{e}$ | $36.2 \pm 17.6^{a}$ | $818 \pm 366^{a}$ | $93.8 \pm 52.1^{a}$ | $3,430 \pm 2,090^{a}$ | $4.27 \pm 4.15$ |
| | | Rad | $1.242 \pm .056^{f}$ | $13.4 \pm 6.5$ | $544 \pm 336^{e}$ | $42.3 \pm 23.9$ | $1,920 \pm 1,310$ | |
| | Strip | Circ | $1.255 \pm .060^{b}$ | $34.1 \pm 16.4^{b}$ | $692 \pm 343^{a}$ | | | |
| | | Rad | $1.478 \pm .095$ | $10.3 \pm 4.8$ | $347 \pm 254$ | | | |

Values are means ± SD. $\lambda^*$, index of leaflet extensibility; $M_{pre}$, $M_{post}$, pre- and posttransitional elastic moduli from membrane analysis; $E_{pre}$, $E_{post}$, pre- and posttransitional elastic moduli from three-dimensional analysis. $^{a,b}P < 0.05, 0.001$, circumferential (Circ) vs. radial (Rad) direction. $^{c,d}P < 0.05, 0.001$, anterior vs. posterior leaflet. $^{e,f}P < 0.05, 0.001$, equibiaxial (Equi) vs. strip biaxial (Strip) protocol.

respectively. Although $R$ for anterior and posterior leaflets did not differ, there were anterior-posterior differences in anisotropy, as judged by the significant differences in circumferential $M_{post}$ (anterior 2,558 vs. posterior 818 N/m), and radial $M_{pre}$ (anterior 801 vs. posterior 544 N/m). However, only circumferential $E_{post}$ remained significantly different between anterior and posterior leaflets (8,960 and 3,430 kPa, respectively) when the three-dimensional analysis was used ($P$ = 0.0436). Thus some but not all of the anterior-posterior differences in anisotropy are attributable to differences in leaflet thickness (see Fig. 6). The differences in extensibility, however, are not related to leaflet thickness.

*Strip biaxial tests.* A comparison between stress-strain results of equibiaxial and strip biaxial (uniaxial) tests in the same specimens provides insight into the effect of multiaxial loading on the mechanical behavior in a particular direction. As depicted in Fig. 7, the circumferential behavior is relatively unaffected by the protocol, exhibiting similar responses whether the transverse direction is equally stretched or unloaded. Results for the uniaxial indexes are shown in Table 2. Compared with the equibiaxial data there were no significant differences in circumferential leaflet properties but highly significant differences in the radial direction. For example, radial $\lambda^*$ increased 41% from 1.183 to 1.34 when tested uniaxially compared with biaxially. Similarly, lower uniaxial radial $M_{pre}$ and $M_{post}$ indicate the mitral tissue behaves as a more extensible material when no strain is applied in the transverse direction.

Posterior leaflet properties reflected trends similar to those of the anterior leaflets in their mechanical behavior when tested with a uniaxial vs. an equibiaxial protocol. The larger extensibility in the radial direction during uniaxial testing was almost double the value for equibiaxial testing, and posttransitional stiffness was significantly decreased, from 555 to 354 N/m ($P$ = 0.0239). All other parameters showed no significant differences.

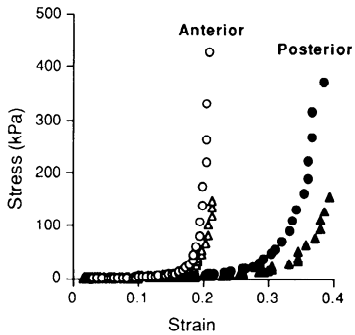


Fig. 6. Three-dimensional stress-strain relations for same specimen shown in Fig. 4. Circles, circumferential direction; triangles, radial direction.

## DISCUSSION

This study is the first to report biaxial mechanical data for mitral valve tissue, thereby establishing a

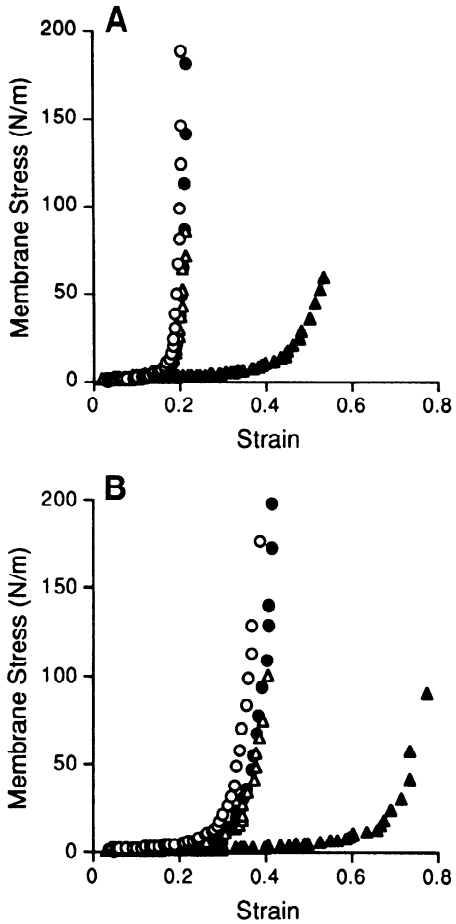


Fig. 7. Membrane stress-strain relations from porcine anterior (*A*) and posterior (*B*) leaflets comparing equibiaxial (open symbols) and strip biaxial (filled symbols) protocols. Circles, circumferential direction; triangles, radial direction.

foundation for the development of a quantitative description of material properties for future stress analyses. The stress-strain relations of excised mitral valve leaflets measured in this study are similar to the nonlinearly elastic properties characteristic of many soft tissues. These results demonstrate that both anterior and posterior mitral valve leaflets exhibit large deformations and behave anisotropically, being stiffer along the circumferential direction. The posterior leaflet is more extensible than the anterior, although their pre- and posttransitional elastic moduli are similar. Comparisons of biaxial vs. uniaxial protocols indicate that circumferential loading strongly affects radial behavior, whereas the converse is not true.

A correlation of this mechanical behavior with known microstructural features will provide a better understanding of the structure-function relationship and guide the future development of a structurally-motivated constitutive law. The two leaflets are asymmetric, with the anterior leaflet broader and roughly triangular and the posterior long and narrow with some natural redundancy when closed (15). Previous studies have demonstrated a higher number of chordal attachments on the posterior compared with the anterior leaflets (15, 18). In humans, the ratio of posterior to anterior chordae is ~1.5 (15, 18), and in pigs this ratio is 1.8 (15). It is reasonable to presume that the total force on a leaflet due to the high systolic ventricular pressure is shared by both the chordae and the leaflet material. Because the anterior leaflet has fewer chordal attachments, the leaflet must thus bear a larger proportion of the force. This may be the reason behind the greater posttransitional stiffness of the anterior leaflet.

Biochemical studies have found that human mitral leaflets are composed of collagen (55–65% dry wt), elastin (10%), and mucopolysaccharides (20%) (1, 5, 23). These components are arranged in three layers: atrialis and/or spongiosa (loosely organized collagen and elastin fibers), fibrosa (dense band of wavy collagen), and ventricularis (endothelium) (7, 28). The mechanical behavior and orientation of the network of collagen and elastin fibers likely determines the mechanical behavior of the tissue. The orientation of collagen fibers in the valve leaflets has been studied previously, and it was demonstrated that collagen fibers are highly oriented along the circumferential axis in the central region of both anterior and posterior leaflets (15). This is probably the reason for the greater stiffness in the circumferential compared with the radial direction.

As in many biological soft tissues containing Type I or III collagen, the fibers in the valve tissue display a crimped configuration (2). The integrated uncrimping of individual collagen fibers with varying amounts of crimping gives rise to a slowly increasing macroscopic elastic modulus until all the fibers are straight and the tissue is quite stiff along the fiber direction. The details of this mechanism are unclear, and several theories have evolved to address this question (19, 20; D. A. MacKenna, and A. D. McCulloch, unpublished observations). However, the results of this study are consistent with predominantly circumferentially oriented crimped collagen fibers, as the circumferential stress-strain relation exhibits a fairly sharp transition from the low modulus region to the stiff posttransitional region. The response of the tissue along the radial axis is greatly altered by the presence of transverse stress and strain, as demonstrated by the difference in stress-strain behavior with equibiaxial vs. strip biaxial stretch protocols. This behavior has been observed in other soft tissues, such as pericardium (Michael Sacks, private communication), and possibly indicates a strong interaction between individual collagen fibers or bundles.

The approach to modeling the constitutive properties of mitral valve tissue should begin by characterizing the tissue as a nonlinear hyperelastic material, similar to other soft biological tissues that exhibit finite deformation. The mitral valve leaflets can be modeled either as thin membranes or as three-dimensional structures that account for differences in leaflet thickness. Treating the leaflets as thin membranes simplifies the mathematics of modeling, reducing the number of independent stress and strain components each from six to three. Although the elastic moduli of the two leaflets are similar using the three-dimensional approach, the posterior leaflet exhibits much greater extensibility than the anterior. Thus, for either membrane or three-dimensional formulations, the anterior and posterior leaflets must be modeled separately as two different materials. Unfortunately, data on the mechanical behavior of each of the layers are lacking.

*Choice of $T^*$.* Fung proposed that the choice of $T^*$ and $\lambda^*$ be physiologically relevant (10). Thus we selected a level of $T^*$ in the posttransitional region to correspond to the predicted peak stress level in the valve tissue during in vivo systolic loading, based on a previous model of the stress in a semicircular membrane clamped at the annular edge and simply supported along the free edge (11). The membrane was assumed to be isotropic and incompressible. An equation for the membrane tension is formulated as a function of applied ventricular systolic pressure, leaflet size, and thickness, and an isotropic operating stiffness. Although this model is greatly simplified compared with the natural mitral valve, it provides an initial estimate of operating stress. Parameters used in this equation were derived from both previous experimental data as well as the present study. Normal transvalvular systolic pressure was estimated to be 110 mmHg (12), the radius of the porcine valve annulus was estimated to be 1 cm (11), and average "isotropic" stiffness values were derived from previous uniaxial data (16). Leaflet thickness values from our study were used. Calculations from these estimates yielded values for anterior and posterior leaflets of 23.0 and 20.4 N/m, respectively; thus a common value of 20 N/m was chosen for $T^*$ for all specimens.

*Comparison with previous work.* All previous studies of the mechanical behavior of mitral valve leaflet tissue have been performed with uniaxial loading (4, 11, 16). Uniaxial tests, however, are not only insufficient for the determination of a constitutive relation (14) but also, as our results demonstrate, do not accurately portray the

behavior of multiaxially loaded tissue. Studies on human anterior leaflets (4, 11) found the transition point in the nonlinear stress-strain relation at 11–14% extension (0.40 kPa stress) (4, 11). Pre- and posttransitional moduli ranged from 10–40 and 200–800 kPa, respectively (4, 11, 16). Our data are consistent with these results, although we chose a different point on the stress-strain curve to tabulate extension and stress at the transition point ($\lambda^*$, $T^*$). In general, the results of these previous studies are similar to our strip biaxial results, demonstrating much larger extensions in the radial than in the circumferential direction (16). Anterior-posterior differences were underestimated, particularly in the radial direction (16), possibly due to disruption of the microstructural fiber network during preparation of the uniaxial test strips, which may not preserve the structural-mechanical properties of the intact leaflet. A correlation of the elastic moduli with the primary collagen fiber orientation in porcine leaflets revealed that the fiber direction is stiffer than the crossfiber direction (16). Our results are consistent with these observations, suggesting that the primary orientation of the collagen fibers in the central region of the valve is circumferential, as has been measured previously (15).

*Relevance to valve function.* The data obtained in this study provide a solid foundation for the quantitative description of material behavior required for any stress analysis in the mitral valve. Previous estimates of peak physiological leaflet stress have used overly simplified material descriptions, relying on a single value for Young's modulus based on the assumption that the posttransitional region is the in vivo operating regime. The peak stress values predicted by these analyses have ranged from 200–20,000 kPa (17, 26, 27), all substantially higher than the estimate obtained from the formula of Ghista and Rao (11) that was used to choose $T^*$ in this investigation. It is difficult to determine whether the predictions of any of these models are accurate, as in vivo stress cannot be reliably measured in the functioning valve. The best alternative is to compare the predicted deformations to measurements of in vivo deformations. There is currently some quantitative information on the shape changes of the valve during the cardiac cycle from cineradiographic and echocardiographic studies. Several of these investigations have revealed significant bulging of the mitral leaflets towards the atrium during systolic contraction (30, 31) and have even documented complex three-dimensional shapes of the mitral complex (21). Observations from these studies suggest that the valve leaflets undergo substantial deformations of 8% or more during peak loading (31). However, the deformations predicted by the stress models are substantially lower ($<3\%$ strain), probably due to the overly simplified and stiff material properties used in these models. Thus the need for both improved stress analyses incorporating more realistic material descriptions as well as the measurement of in vivo deformations for model validation in the mitral valve should guide future efforts in this field.

These data could also be used to guide the development of bioprosthetic valve substitutes. It is probably desirable to mimic the natural mitral valve mechanical properties when designing bioprostheses for repair or replacement, thus detailed quantification of the normal biomechanical properties provides needed information for biologists and engineers involved in this design process.

*Study limitations.* Ideally, the stress-strain properties of a tissue would be obtained from in vivo testing; however, in most tissues this is not possible. The properties of excised tissue may closely reflect the in vivo properties if the tissue is tested fresh and deterioration of tissue structure is minimized. In this study, we were unable to test all specimens fresh; however, the changes induced by saline storage for a few days were assessed and found to be minimal. Thus we are confident that the stress-strain properties reflect those of the natural tissue with reasonable accuracy.

The tissue was stretched until it exhibited rapid stiffening, which occurred at different stretch limits in different leaflet specimens. We desired to obtain data in the full nonlinear range, including a substantial portion of the posttransitional region. The maximum levels of stretch applied reflected this, and were not indicative of the maximum values the tissue might experience in testing to failure. We were concerned that ultrastructural tissue damage might occur if high stresses were produced, as the posttransitional region exhibits high stress changes with small increases in stretch. To minimize this potential problem, we evaluated the cycle-to-cycle repeatability for each protocol, and data that did not demonstrate this were discarded.

In these experiments, the valve leaflet properties were measured at a relatively low strain rate of 4–12%/s. Extrapolation of the stress-strain behavior of tissues measured at one strain rate to a much different strain rate should be performed carefully, taking into account any viscous properties of tissue behavior. The actual in vivo strain rate of the mitral leaflets is not precisely known, as strain during systolic loading has not been accurately quantified. Estimates based on mathematical models and cineradiographic images indicate that strain rate during physiological loading may range from 20–80%/s (17, 31), two to twenty times greater than the rate used in our study. To address this issue, additional tests were performed on two leaflets in which identical protocols were applied over a wide range of strain rates: 0.5–40%/s. The results from these tests show remarkably similar mechanical responses over the entire range, indicating valve tissue is fairly insensitive to strain rate, as has been observed previously (data not shown) (16). As the valve tissue is composed primarily of elastin and collagen, which individually demonstrate predominantly elastic behavior, one would not expect a large viscoelastic effect (9).

Shearing strains can significantly affect the calculation of stresses in a biaxial experiment. With our analysis procedure, we can calculate shearing strains and stresses off-line after the experiment but cannot control for them during the actual test. Thus we evalu-

ated the shear contributions postexperimentally to determine whether they significantly affected our results. We found that the shearing strains and accompanying stresses were small but not identically equal to zero. However, they were small enough to be considered negligible in the data reported. Another potential source of error in the calculation of Cauchy (three-dimensional) stresses is the measurement of undeformed leaflet thickness. This measurement is difficult to make accurately, as it is uncertain whether the caliper tips are deforming the tissue and distorting the measurement. In this study, leaflet thickness was carefully measured three times and averaged for each specimen. The precision of this measurement is $\sim 0.03$ mm, which translates to an error of $\leq 6\%$ in the calculation of Cauchy stress.

For the analysis of our equibiaxial data, we excluded tests in which there was a 10% or larger deviation from the prescribed equibiaxial stretch ratio. Deviations from the prescribed protocol were most likely due to shearing behavior that was not revealed until postexperimental data analysis or slight inaccuracies in the identification of the marker centroids. The strain data presented in the results were calculated from the locations of the individual markers, whereas the servo control during the experiment was based on a more approximate displacement of the markers calculated as the average distance between marker pairs. Therefore, the strain results reported are a more accurate representation of the actual mechanical behavior during the experiment than the displacement values used to control the applied stretch waveform.

Although anterior-posterior leaflet variations were assessed in this study, more complex regional variations in mitral mechanical properties likely exist in the normal valve. Structural inhomogeneities, such as those near the chordae tendineae insertion sites, are probably associated with local variations in mechanical properties. Previous comparisons of leaflet properties to those of the chordae tendineae reveal chordae behaves as a much stiffer material, with a lower extension and a higher stress at the transition point and higher elastic moduli in both regions (4, 16). These detailed regional variations in mechanical properties were not assessed in this study and merit further investigation.

In conclusion, mitral valve leaflets are anisotropic, nonlinear elastic tissues capable of large (10–60%) deformations before reaching physiological stress levels. The stress-strain behavior along the circumferential direction is substantially stiffer than along the radial direction, most likely due to the circumferential orientation of stiff, wavy collagen fibers in the central region of the leaflets. Anterior and posterior leaflets displayed quantitatively different behavior, with posterior leaflets demonstrating greater extensibility and lower elastic moduli than anterior leaflets. These differences may be explained by the greater number of chordae insertion sites on the posterior leaflet, which provide additional mechanical stability to this leaflet. Variations in the stress-strain response with different stretch protocols indicate a strong effect of circumferential stress and strain on radial material properties and may be related to microstructural tethering between collagen fibers or bundles. Knowledge of the mechanical behavior of mitral valve tissue is necessary in the assessment of physiological stress, and may provide information for the development of improved bioprosthetic substitutes. The data from this study provide a foundation for the development of a quantitative material description, which must agree both qualitatively and quantitatively with the results presented in this paper.

The authors gratefully acknowledge the assistance of Kristi Pier, Michael Samphilipo, Carolyn Magee, Taewon Kang, and Eric C. Burdge in performing the experiments. We also thank Michael Sacks for insightful discussions on the interaction between valve structure and function.

This work was supported by National Heart, Lung, and Blood Institute Grants HL-33621 and T32 HL-07227.

Address for reprint requests: K. May-Newman, Johns Hopkins Univ., 930 Traylor Bldg., 1721 E. Madison St., Baltimore, MD 21205.

Received 19 December 1994; accepted in final form 11 April 1995.

## REFERENCES

1. **Bashey, R. I., and S. A. Jimenez.** Collagen in heart valves. In: *Collagen*, edited by M. Nimni. Boca Raton, FL: CRC Press, 1988, p. 273–292.
2. **Broom, N. D.** Simultaneous morphological and stress-strain studies of the fibrous components in wet heart valve leaflet tissue. *Connect. Tissue Res.* 6: 37–50, 1978.
3. **Chew, P. H., F. C. P. Yin, and S. L. Zeger.** Biaxial stress-strain properties of canine pericardium. *J. Mol. Cell. Cardiol.* 18: 567–578, 1986.
4. **Clark, R. E.** Stress-strain characteristics of fresh and frozen human aortic and mitral leaflets and chordae tendineae. *J. Thorac. Cardiovasc. Surg.* 66: 202–208, 1973.
5. **Cole, W. G., D. Chan, A. J. Hickey, and D. E. Wilcken.** Collagen composition of normal and myxomatous human mitral heart valves. *Biochem. J.* 219: 451–460, 1984.
6. **Collins, D., K. Lindberg, B. McLees, and S. Pinnell.** The collagen of heart valve. *Biochim. Biophys. Acta* 495: 129–139, 1977.
7. **Cooper, T., L. M. Napolitano, M. J. T. Fitzgerald, K. E. Moore, W. M. Daggett, V. L. Willman, E. H. Sonnenblick, and C. R. Hanlon.** Structural basis of cardiac valvar function. *Arch. Surg.* 93: 767–771, 1966.
8. **Downs, J., H. R. Halperin, J. Humphrey, and F. Yin.** An improved video-based computer tracking system for soft biomaterial testing. *IEEE Trans. Biomed. Eng.* 37: 903–907, 1990.
9. **Fung, Y. C.** *Biomechanics: Mechanical Properties of Living Tissues*. New York: Springer-Verlag, 1981, chapt. 7, p. 196–260.
10. **Fung, Y. C. B.** Elasticity of soft tissues in simple elongation. *Am. J. Physiol.* 213: 1532–1544, 1967.
11. **Ghista, D. N., and A. P. Rao.** Mitral-valve mechanics–stress/strain characteristics of excised leaflets, analysis of its functional mechanics and its medical application. *Med. Biol. Eng.* 11: 691–701, 1973.
12. **Guyton, A. C.** *Textbook of Medical Physiology* (7th ed.). Philadelphia, PA: Saunders, 1986.
13. **Humphrey, J. D., D. L. Vawter, and R. P. Vito.** Quantification of strains in biaxially tested soft tissues. *J. Biomech.* 20: 59–65, 1987.
14. **Humphrey, J. D., and F. C. P. Yin.** On constitutive relations and finite deformations of passive cardiac tissue: I. A pseudostrain-energy function. *J. Biomech. Eng.* 109: 298–304, 1987.
15. **Kunzelman, K. S.** *Engineering Analysis of Mitral Valve Structure and Function* (PhD thesis). Dallas, TX: Univ. of Texas Southwestern Medical Center, 1991.
16. **Kunzelman, K. S., and R. P. Cochran.** Stress/strain characteristics of porcine mitral valve tissue: parallel versus perpendicular collagen orientation. *J. Cardiol. Surg.* 7: 71–78, 1992.
17. **Kunzelman, K. S., R. P. Cochran, C. Chuong, W. S. Ring, E. D. Verrier, and R. D. Eberhart.** Finite element analysis of the mitral valve. *J. Heart Valve Dis.* 2: 326–340, 1993.

18. **Lam, J. H. C., N. Ranganathan, E. D. Wigle, and M. D. Silver.** Morphology of the human mitral valve: I. Chordae tendineae: a new classification. *Circulation* 41: 449–458, 1970.
19. **Lanir, Y.** A structural theory for the homogeneous biaxial stress-strain relationships in flat collagenous tissues. *J. Biomech.* 12: 423–436, 1979.
20. **Lanir, Y.** Constitutive equations for fibrous connective tissues. *J. Biomech.* 16: 1–12, 1983.
21. **Levine, R. A., M. D. Handschumacher, A. J. Sanfilippo, A. A. Hagege, P. Harrigan, J. E. Marshall, and A. E. Weyman.** Three-dimensional echocardiographic reconstruction of the mitral valve, with implications for the diagnosis of mitral valve prolapse. *Circulation* 80: 589–598, 1989.
22. **Lim, K. O., and D. R. Boughner.** Mechanical properties of human chordae tendineae. *Can. J. Physiol. Pharmacol.* 53: 332–339, 1975.
23. **Lis, Y., M. C. Burleigh, D. J. Parker, A. H. Child, J. Hogg, and M. J. Davies.** Biochemical characterization of individual normal, floppy and rheumatic human mitral valves. *Biochem. J.* 244: 597–603, 1987.
25. **Mayne, A. S. D., G. W. Christie, B. H. Smaill, P. J. Hunter, and B. G. Barratt-Boyes.** An assessment of the mechanical properties of leaflets from four second-generation porcine bioprostheses with biaxial testing techniques. *J. Thorac. Cardiovasc. Surg.* 98: 170–180, 1989.
26. **Mazumdar, J., and T. C. Hearn.** Mathematical analysis of mitral valve leaflets. *J. Biomech.* 11: 291–296, 1978.
27. **Miller, G. E., and H. Marcotte.** Computer simulation of human mitral valve mechanics and motion. *Comput. Biol. Med.* 17: 305–319, 1987.
28. **Mitomo, Y., K. Nakao, and A. Angust.** The fine structure of the heart valves in the chicken. *Am. J. Anat.* 125: 147–168, 1969.
29. **Nielsen, P. M. F., P. J. Hunter, and B. H. Smaill.** Biaxial testing of membrane biomaterials: testing equipment and procedures. *J. Biomech. Eng.* 113: 295–300, 1991.
30. **Rushmer, R. F., B. L. Finlayson, and A. A. Nash.** Movements of the mitral valve. *Circ. Res.* 4: 337–342, 1956.
31. **Sovak, M., P. R. Lynch, and G. H. Steward.** Movement of the mitral valve and its correlation with the first heart sound. *Invest. Radiol.* 8: 150–155, 1973.
32. **Strumpf, R. K., J. D. Humphrey, and F. C. P. Yin.** Biaxial mechanical properties of passive and tetanized canine diaphragm. *Am. J. Physiol.* 265 (*Heart Circ. Physiol.* 34): H469–H475, 1993.